East European Journal of Physics. 3. 422-430 (2025)
DOI:10.26565/2312-4334-2025-3-45 ISSN 2312-4334

SEMI-EMPIRICAL MODELS OF ELECTRON BEAM CONTROL FOR RADIATION STERILIZATION

Igor O. Girka, Valentin T. Lazurik*
V.N. Karazin Kharkiv National University, Kharkiv, Ukraine
**Corresponding Author e-mail: vtlazurik@karazin.ua*
Received May 17, 2025; revised July 13, 2025; accepted August 15, 2025

To carry out radiation sterilization, one needs to determine the permissible irradiation modes, which is carried out using computer dosimetry methods. Nowadays, the choice of optimal irradiation modes can be based on the models of the depth-dose curve at different incidence angles of the electron beam on the layer of matter. In the present paper, the distribution of transferred energy in the volume of the target initiated by the normal incidence of a point beam of radiation on the surface of a semi-infinite medium (***Dose-Map*** object) is used to develop such models. Semi-empirical models of the ***Dose-Map*** object are designed based on two assumptions. One is that the target has axial symmetry relative to the direction of the radiation particle incidence on the target. The second is that the dose spatial distribution is uniform or normal (Gaussian distribution) in the cross-sections of the ***Dose-Map*** object at all depths. For a two-parameter approximation of the ***Dose-Map*** object, three-dimensional geometric figures are suggested, which surfaces are formed by rotating the plots of power functions around the abscissa axis. Semi-empirical models are developed based on the assumption that the parameters of the ***Dose-Map*** object in its eigen coordinate system do not change when the beam incidence angle changes. Expressions are obtained for calculating the depth-dose curves from radiation incident on the target at an angle θ in the form of an integral transformation of the depth-dose curve for normal incidence of the radiation beam on the target. Software has been developed for calculating depth-dose curves in a semi-infinite medium under uniform irradiation by an electron beam. The implemented algorithms for calculating the depth-dose curves from an electron beam incident on the target at the angle θ are tested. Satisfactory agreement is established between the results obtained using the developed semi-empirical models and the results of Monte Carlo modeling of the depth-dose curves at different incidence angles of the electron beam on the target. Good agreement is established between the results obtained using the semi-empirical model "***Cone***" and the results obtained using the developed two-parameter semi-empirical models ***SEM2U*** and ***SEM2N***. The capabilities of the developed two-parameter models for a more complete description of the technological characteristics of the radiation sterilization process are investigated using the numerical methods. Examples are provided where the developed two-parameter models allow for the simultaneous description of two technological characteristics of the two-sided irradiation process: the optimal target thickness and the dose uniformity ratio (***DUR***) in the target. Consistent data on these characteristics allow choosing optimal modes of electron beam irradiation during radiation sterilization in a reasonable manner. The possibilities of using the approach suggested in the present paper for developing a set of semi-empirical models of computer dosimetry of irradiation processes in radiation technologies are noted.
Keywords: *Electron beam dosimetry; Depth-Dose curve; Sterilization processes; Control of optimal modes; Semi-empirical model; Monte-Carlo method*
PACS: 87.53.Bn, 02.60.Cb

INTRODUCTION

The tasks of optimizing irradiation processes arose simultaneously with the introduction of radiation technologies [1-11]. Optimization of irradiation processes is ensured by minimizing the level of non-uniformity of the irradiation dose in the volume of the target being processed [12-20]. For electron beams, the method of two-sided irradiation provides high uniformity of the irradiation dose in the layer [4, 5]. The effective application of this method needs the irradiated layer to be of an optimal thickness H_{opt}, which is determined from the condition of equality of the minimum dose value in the center of the layer to the dose value at the boundary of the layer. For the fixed thickness of the irradiated layer, a strong dependence of the ratio $DUR = D_{max}/D_{min}$ on the electron energy is observed. Here D_{max} is the maximum dose value, and D_{min} is the minimum dose value. This dependence causes difficulties in planning and controlling the irradiation process, which are associated with technical problems arising from the need to vary the electron energy.

Varying the angle of the electron beam incidence on the irradiated object surface is considered as a possible solution to technical problems in implementing the two-sided irradiation method [21-27]. Figure 1 shows the depth-dose curves in polyethylene layers of fixed mass thickness H_1 = 8.25 g/cm^2 and H_2 = 6.06 g/cm^2 under two-sided irradiation with electron beams. The doses under normal incidence of an electron beam with energy E = 10 MeV are shown by red dashed curves. The dose in the H_1 layer for the incidence angle of $\theta_1 = 20^0$ of the electron beams with the energy E = 10 MeV an as well as that in the H_2 layer at the incidence angle of $\theta_2 = 45^0$ are given by the black dashed curves, both are calculated in the semi-empirical model [23]. The beam incidence angles for each layer are selected to provide the optimal thicknesses for two-sided irradiation. The results of Monte Carlo simulation of depth-dose curves are presented in Fig. 1 by solid curves for comparison [12,13]. The depth-dose curves for normal incidence of an electron beam with energy E_1 = 9.3 MeV on the H_1 layer as well those for an electron beam with energy E_2 = 6.9 MeV incidence on the H_2 layer are shown by

Cite as: I.O. Girka, V.T. Lazurik, East Eur. J. Phys. 3, 422 (2025), https://doi.org/10.26565/2312-4334-2025-3-45

dotted curves. For each layer, the electron energy is chosen in such a way that the layer thickness is the optimal one for two-sided irradiation.

One can see in Fig. 1, that the dose non-uniformity ***DUR*** at normal incidence of an electron beam with an energy of 10 MeV (see red dashed curves) can significantly exceed the dose non-uniformity during irradiation with electrons with a specially selected energy (which is the essence of optimization method 1) or with a specially selected beam incidence angle (which is the essence of optimization method 2).

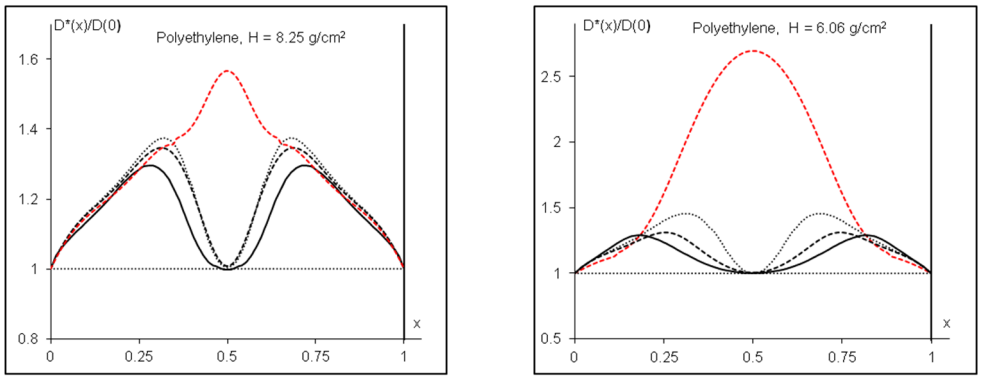

Figure 1. Depth-dose curves for two-sided irradiation of a layer of fixed thickness *H*

Comparison of ***DUR*** values in layers of fixed thickness under electron irradiation using optimization method 1 (dotted curves) with those calculated using optimization method 2 (black dashed curves) shows that optimization method 2 provides more uniform dose distribution in the layer. Let compare also the Monte Carlo simulation of the depth-dose curves, presented in Fig.1 by solid curves, with the results calculated within the semi-empirical model (black dashed curves). One can see that the errors in calculating the ***DUR*** values within the semi-empirical model can be significant.

Therefore, further development of models and methods for describing depth-dose curves at different incidence angles of the electron beam on the layer of matter is the actual problem. The development is necessary when using method 2 to optimize the irradiation parameters in the practical implementation of radiation sterilization.

Development of models and methods for implementing the optimization method 2 was presented in [23-27]. The Monte Carlo method based on the detailed physical model was used in [13] to simulate the depth-dose curves for different incidence angles of the electron beam on the layer. Unfortunately, large arrays of numerical data were the key results of the modeling. These arrays are of little use in searching for optimal irradiation parameters for the practical activities of radiation sterilization centers. Semi-empirical models of the depth-dose curve were developed in [23, 27] for a limited range of incidence angles of the electron beam on the layer. The distribution of the transferred energy in the volume of the target, initiated by the passage of one particle of radiation through the target, was considered as the basic object of the model (the ***Dose-Map*** object) in the development of these models. Since the passage and transfer of energy by a radiation particle to a substance is a stochastic process, the ***Dose-Map*** is defined as the average value of the dose distribution over a large number of radiation particles. The semi-empirical model was presented in [27], in which the geometric shape of a cone with one adjustable parameter, the cone angle, was used to approximate the ***Dose-Map*** object. The model parameter was determined in the result of fitting the data calculated using the semi-empirical model to the data obtained by Monte Carlo simulation in a detailed physical model. For example, for the ISE model [27], the model parameter was determined using data on the optimal layer thicknesses at different incidence angles of the electron beam on the layer [23]. Note that application of single-parameter semi-empirical models, unfortunately, can provide a good description of only one of the technological indicators of the irradiation.

In the present paper, two-parameter semi-empirical models are suggested that can simultaneously describe the optimal layer thickness and the dose uniformity index ***DUR*** for two-sided irradiation. This is necessary to make a decision on the appropriateness of using irradiation parameters to carry out the radiation sterilization. To design such models, a generalized model of the Dose-Map object is developed at the first stage of the present research, which can ensure the elaboration of semi-empirical models for the depth-dose curve in a semi-infinite medium at a given incidence angle of radiation particles on the target.

DISTRIBUTION OF ENERGY TRANSFERRED FROM ONE RADIATION PARTICLE TO THE TARGET VOLUME

Let us start with considering the case of normal incidence of radiation particles on a semi-infinite medium. The material of the medium is assumed to be isotropic with respect to the processes of passage and scattering of particles in the medium. In this case, the distribution of energy transferred from one radiation particle to the target volume (***Dose-Map*** object) has axial symmetry relative to the direction of incidence of the radiation particle (***X*** axis) on the medium. To determine the parameters of the ***Dose-Map*** object model, the well-known fact is applied, that with uniform irradiation of the surface of the medium, the dose at any depth ***x*** in the medium is proportional to the integral value of the energy released in the cross-section of the ***Dose-Map*** object by the plane at depth ***x***. This means that if the flux of radiation

particles $\boldsymbol{\Phi(y,z)}$ incident on the surface (x=0) does not depend on the coordinates ($\boldsymbol{y,z}$) along the surface ($\boldsymbol{\Phi(y,z) \equiv \Phi_0}$), then the dependence of the depth-dose curve $\boldsymbol{D(x)}$ on the depth $\boldsymbol{x}$ in the medium is determined by the expression [27]

$$D(x) = \Phi_0 \int\limits_{G(x)} D_p(x, y.z) \cdot dS\,, \qquad dS = dydz\,, \tag{1}$$

where $\boldsymbol{D_p(x,y,z)}$ is the dose distribution in the volume of the medium, which is produced by one radiation particle entering the medium, i.e. the mathematical description of the ***Dose-Map*** object. $\boldsymbol{G(x)}$ is the cross-section of the ***Dose-Map*** object at depth $\boldsymbol{x}$. Relation (1) makes it possible to determine the integral values of the dose $\boldsymbol{E(x)}$ in the cross-section $\boldsymbol{G(x)}$ of the ***Dose-Map*** object based on the data on the depth-dose curve under uniform irradiation of the surface of the medium

$$E(x) \equiv D(x)/\Phi_0. \tag{2}$$

Note that relations (1) and (2) are valid for radiation fluxes of any type and for any angles of incidence of a radiation particle on the boundary of the medium. Therefore, the depth-dose curve $\boldsymbol{D(x,\theta)}$ from the radiation entering the medium at an angle $\boldsymbol{\theta}$ can be calculated based on the integral value of the dose $\boldsymbol{E(x,\theta)}$ in the cross-section $\boldsymbol{G(x,\theta)}$ in accordance with the following expressions

$$E(x,\theta) = \int\limits_{G(x,\theta)} D_p(x, y.z, \theta) \cdot dS\,, \quad dS = dydz\,, \tag{3}$$

$$D(x,\theta) = \Phi_0 \cdot E(x,\theta)\,,$$

where $\boldsymbol{D_p(x,y,z,\theta)}$ is the dose distribution in the volume of the medium, which is produced by one radiation particle entering the medium at an angle $\boldsymbol{\theta}$.

The depth-dose curves for uniform irradiation of a semi-infinite medium for particles of various types of radiation (electrons, gamma quanta, protons, X-rays) falling normally on the surface of the medium have been studied in detail. For example, for electron irradiation, a semi-empirical model [28] and the implementation of the program for calculating the depth-dose curves in various materials are known. Therefore, for electron irradiation, the integral values of the dose $\boldsymbol{E(x)}$ can be calculated according to (2), based on these data. Therefore, to complete the stage of determining the parameters of the ***Dose-Map*** object, it is sufficient to establish the characteristics of the dose distribution in the cross-sections $\boldsymbol{G(x)}$ at all depths $\boldsymbol{x}$ in the target.

Uniform distribution and normal (Gaussian) distribution are the simplest types of distribution. Due to the axial symmetry of the ***Dose-Map*** object, to describe the uniform distribution it is sufficient to know the dependence of the radius $\boldsymbol{R(x)}$ of the circle on the depth x in the medium. The Gaussian distribution requires the variance $\boldsymbol{\sigma(x)}$ to depend on the depth $\boldsymbol{x}$ in the medium. These dependencies should be described by continuous positive functions.

In the present paper, power functions are used as model dependences of dose distributions on x in cross-sections of the ***Dose-Map*** object:

$$F(x) = \alpha \cdot L_{\max} \left(\frac{x}{L_{\max}} \right)^{Q}, \qquad Q \geq 0, \quad 0 < x \leq L_{\max}\,. \tag{4}$$

In (4), $\boldsymbol{L_{max}}$ is the path depth of the radiation particles in the medium [4]. Thus, the ***Dose-Map*** object model is completely formed and has two model parameters. First, $\boldsymbol{\alpha}$ determines the maximum value of the function $\boldsymbol{F_{max} = \alpha * L_{max}}$. And, second, $\boldsymbol{Q}$ is the exponent of the power function.

DEPTH-DOSE CURVES FOR A GIVEN ANGLE OF INCIDENCE OF RADIATION PARTICLES ON A SEMI-INFINITE MEDIUM

Basic assumptions in developing semi-empirical models

The statement that the parameters of the Dose-Map object in its eigen coordinate system [$\boldsymbol{x^*, y', z'}$] do not change with a change in the angle $\boldsymbol{\theta}$ is the main assumption in developing the semi-empirical models. This assumption obviously is valid only for those angles $\boldsymbol{\theta}$, for which the influence of the boundary of the target on the dose distribution in the Dose-Map object can be neglected.

As follows from (3), to calculate the depth-dose curve $\boldsymbol{D(x,\theta)}$ in a medium from radiation incident at an angle $\boldsymbol{\theta}$, it is sufficient to calculate the integral values of the dose $\boldsymbol{E(x,\theta)}$ in the section $\boldsymbol{G(x,\theta)}$ of the dose distribution $\boldsymbol{D_p(x,y,z,\theta)}$ (see Fig. 2). To determine the magnitude of the integral dose values $\boldsymbol{E(x,\theta)}$ in the region $\boldsymbol{G(x,\theta)}$, the contributions $\boldsymbol{\Delta(x,x^*,\theta)}$ are integrated from each of the regions $\boldsymbol{G(x^*,\theta)}$, which are located perpendicular to the $\boldsymbol{X^*}$ axis from $\boldsymbol{x^*}$= 0 of the boundary of the medium to $\boldsymbol{x^* = L_{max}}$ of the maximum depth of the ***Dose-Map*** object. Then, the relation (3) for the depth-dose curve $\boldsymbol{D(x,\theta)}$ from the radiation entering the medium at an angle $\boldsymbol{\theta}$ read

$$D(x,\theta) = \Phi_0 \int\limits_{0}^{L_{\max}} \Delta(x, x^*, \theta) dx^*\,. \tag{5}$$

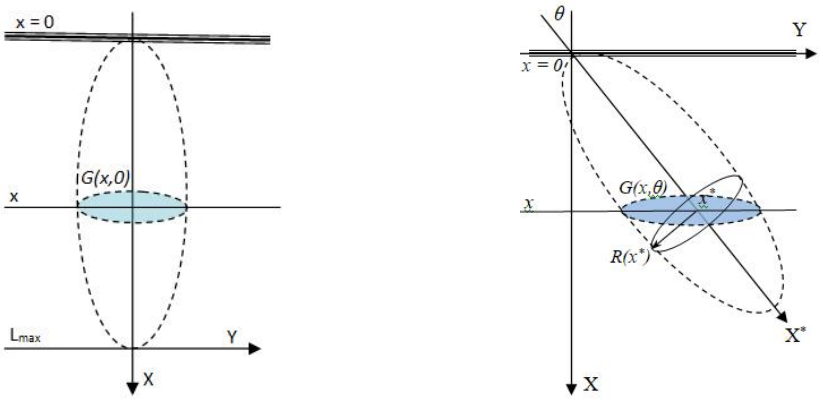

Figure 2. A model of the distribution of transferred energy in a volume of the target, which is initiated by the passage of one particle of radiation through the matter - a ***Dose-Map*** object

Uniform dose distribution in the cross-sections of the *DOSE-MAP* object

For a uniform dose distribution in the sections of the Dose-Map object, the dependence of the radius ***R(x)*** in the cross sections ***G(x,0)*** on the depth ***x*** in the medium is assumed to be known. Then the conditions of intersection of the region ***G(x*, 0)*** with the plane perpendicular to the ***X*** axis at the depth ***x*** in the medium are check while integrating eq. (5)

$$h(x,x^*) < R(x^*), \quad h(x,x^*) = \frac{x - x^* \cdot \cos(\theta)}{\sin(\theta)}, \tag{6}$$

where ***h(x,x*)*** is the distance from point x^* on the plane perpendicular to the X^* axis to the line of intersection of this plane with the plane perpendicular to the ***X*** axis at the depth ***x*** in the medium (see Fig. 3).

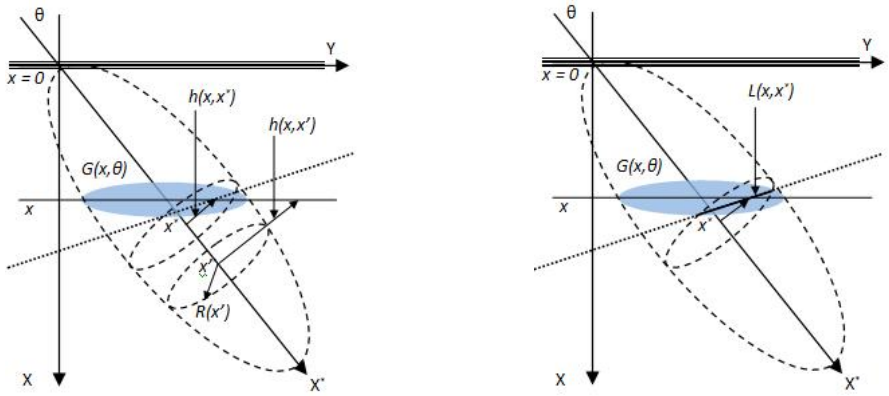

Figure 3. To calculating the depth-dose curve in a semi-infinite medium.

If condition (6) is met, then the contribution of the region $G(x^*,0)$ to the dose value in the region $G(x^*,\theta)$ is proportional to the chord length $L(x,x^*)$ (see Fig. 3):

$$L(x,x^*) = 2 \cdot \sqrt{R^2(x^*) - h^2(x,x^*)}\,. \tag{7}$$

In accordance with the assumption that the parameters of the ***Dose-Map*** object in its eigen coordinate system $[x^*,y',z']$ do not change with a variation of the angle θ, the dose distribution in the medium $D_p(x^*,y',z',\theta)$ can be represented as

$$D_p(x^*,y',z',\theta) \equiv \begin{cases} \dfrac{E(x^*)}{\pi R^2(x^*)} & y'^2 + z'^2 \le R^2(x^*) \\ 0 & y'^2 + z'^2 > R^2(x^*) \end{cases},$$

$$E(x) = \int\limits_{G(x)} D_p(x,y.z)dS, \quad dS = dydz\,, \tag{8}$$

where $R(x)$ is the radius of the section $G(x)$ of the ***Dose-Map*** object. In this case, the contribution $\Delta(x,x^*,\theta)$ from the region $G(x^*,0)$ of the ***Dose-Map*** object to the region $G(x,\theta)$ reads

$$\Delta(x,x^*,\theta)=\frac{E(x^*)}{\pi R^2(x^*)}\cdot\frac{L(x,x^*)}{\sin(\theta)}. \tag{9}$$

In (9), the multiplier $1/\sin(\theta)$ determines the effective area of intersection of the plane perpendicular to the X^* axis at point x^* with the plane perpendicular to the X axis at depth x in the medium.

According to (5), the depth-dose curve $D(x,\theta)$ from radiation entering the medium at an angle θ is determined by the relation

$$D(x,\theta)=\Phi_0\int_0^{L_{\max}}\frac{E(x^*)}{\pi R^2(x^*)}\cdot\frac{L(x,x^*)}{\sin(\theta)}dx^*. \tag{10}$$

This relationship can easily be represented as an integral transformation of the depth-dose curve $D(x,0)$ from radiation entering the medium at an angle 0°.

$$D(x,\theta)=\frac{1}{\pi\sin(\theta)}\int_0^{L_{\max}}D(x^*,0)\cdot\frac{L(x,x^*)}{R^2(x^*)}dx^*. \tag{11}$$

Note that in (11), the dependence $R(x)$ can be any continuous positive function. In particular, when choosing $R(x)\equiv R_0$, one obtains the model "Cylinder". If one chooses $R(x)\equiv x\cdot\tan(\omega)$, the equivalent of the model "Cone" [27] is obtained. In the present paper, the two-parameter model of the Dose-Map object is applied, $R(x)\equiv F(x)$ (see eq. (4)), and two-parameter (α,Q) semi-empirical model SEM2U is designed for the depth-dose curve in a semi-infinite medium at a given incidence angle of electrons on the medium.

Normal dose distribution in cross-sections of the DOSE-MAP object

For a normal dose distribution in the cross-sections of the Dose-Map object, the dependence of the variance $\sigma(x)$ of the distribution in the cross-sections on the depth x in the medium is assumed to be known. This model uses a dose distribution in the cross-sections of the Dose-Map of the type of axially symmetric spatial distribution of the Gaussian type on a plane, i.e.

$$D_p(x^*,y',z',\theta)\equiv\frac{E(x^*)}{2\pi\sigma^2(x^*)}\cdot e^{\frac{-(y'^2+z'^2)}{2\sigma^2(x^*)}}, \tag{12}$$

$$E(x)=\int_{G(x)}D_p(x,y.z)dS,\qquad dS=dydz,$$

where $\sigma(x)$ is the dependence of the variance of the dose distribution in the ***Dose-Map*** cross sections on the depth x in the medium; x^*, y', z' are the coordinates of the ***Dose-Map*** object in its eigen coordinate system.

For a normal dose distribution in the cross-sections of the ***Dose-Map*** object, the contribution from the region $G(x^*,0)$ to the dose value in the region $G(x,\theta)$) can be determined by integrating the contributions along the line of intersection of the plane perpendicular to the X^* axis at point x^* with the plane perpendicular to the X axis at depth x (see Fig. 3, dotted line).

According to the basic assumptions, the ***Dose-Map*** object has axial symmetry relative to the direction of incidence of the radiation particle (axis X^*) on the target and in its eigen coordinate system does not change when the incidence angle of the radiation particle varies. Therefore, one can choose the Z' axis parallel to the dotted line - the intersection of the planes shown in Fig. 3. Note that with this choice of coordinate system orientation, the Y' axis is perpendicular to the intersection line of the planes. In this case, the contribution $\Delta(x,x^*,\theta)$ from the region $G(x^*,0)$ of the ***Dose-Map*** object to the region $G(x,\theta)$ can be represented as follows

$$\Delta(x,x^*,\theta)=\frac{1}{\sin(\theta)}\int_{-\infty}^{+\infty}D_p(x^*,y',z',\theta)dz'. \tag{13}$$

Using (12) and integrating in eq. (13), one obtains

$$\Delta(x,x^*,\theta)=\frac{1}{\sqrt{2\pi}\cdot\sin(\theta)}\frac{E(x')}{\sigma(x^*)}e^{\frac{-h^2(x,x^*,\theta)}{2\sigma^2(x^*)}}, \tag{14}$$

where $h(x,x^*,\theta)$ is the distance along the Y' axis to the intersection line of the planes.

According to (5), for the depth-dose curve $D(x,\theta)$ from radiation entering the medium at an angle θ, we have the relation

$$D(x,\theta)=\frac{1}{\sqrt{2\pi}\cdot\sin(\theta)}\int_0^{L_{max}}\frac{D(x^*)}{\sigma(x^*)}\cdot e^{-\frac{h^2(x,x^*,\theta)}{2\sigma^2(x^*)}}dx^*\ . \qquad (15)$$

In this version of the computational scheme, the dependence $\sigma(x)$ can be chosen as an arbitrary continuous positive function. However, ensuring a given error in the calculation results requires numerical methods that take into account the features of the chosen dependence. In the present paper, two-parameter model of the Dose-Map object, $\sigma(x)\equiv F(x)$ (see eq. (4)) is used, and two-parameter (α,Q) semi-empirical model SEM2N is designed for the depth-dose curve in a semi-infinite medium at a given incidence angle of electrons on the medium.

NUMERICAL STUDY OF TWO-PARAMETER EMPIRICAL MODELS

Study of two-parameter SEM2U model

Software for calculating depth-dose curves using the SEM2U model is developed. The calculation results obtained using the SEM2U model are compared with those obtained using the "Cone" model. To do this, one has to take the model parameter Q = 1, and the value of the parameter α is determined by the value of the parameter ω of the "Cone" model, α = tan(ω). For the angles θ ≤ 60°, when the influence of the medium boundary on the dose distribution in the Dose-Map object can be neglected, good agreement between the calculation results obtained using these models is observed. It should be noted that the observed differences are associated only with the error in the numerical integration of the relationships for calculating the depth-dose curve in a semi-infinite medium.

Figure 4 shows the depth-dose curves in a semi-infinite medium and in a layer with two-sided irradiation. The black solid curves correspond to the calculations in the "Cone" model and the SEM2U model with the model parameters Q_u = 1, α_u=0.47. Dotted curves relate to the calculations in the SEM2U model with the model parameters: Q_u=1.5, α_u=0.53 (curve 1); Q_u=1.1, α_u=0.55 (curve 2); Q_u=0.9, α_u=0.40 (curve 3); and Q_u=0.5, α_u=0.65 (curve 4). Red solid curves are calculated in the result of modeling the depth-dose curves using the Monte Carlo method.

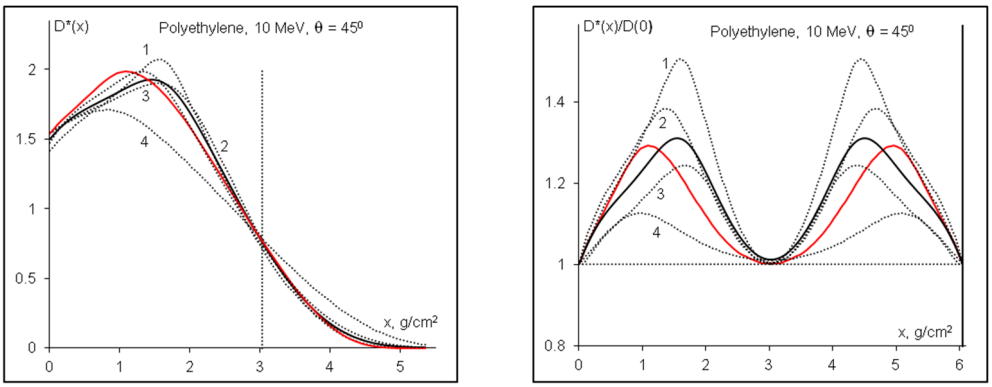

Figure 4. Depth-dose curves in a semi-infinite medium (left) and in a layer of optimal thickness H_{opt} = 6.06 g/cm² with two-sided irradiation (right).

One can see in Fig. 4, that the selected combinations of model parameter values (Q,α) describe a set of depth-dose curves for which the value of the optimal layer thickness for two-sided irradiation is fixed. At the same time, the value of the dose distribution uniformity characteristic DUR in this set varies in a wide range – from 1.1 to 1.5. This confirms that in the two-parameter SEM2U model, it is possible to select the values of the model parameters in such a way that the calculated depth-dose curves simultaneously describe two technological characteristics of the irradiation.

Study of two-parameter SEM2N model

Software for calculating depth-dose curves using the SEM2N model is produced. The calculation results obtained using the SEM2N model are compared with those obtained using the "Cone" model. Figure 5 shows the depth-dose curves calculated in the "Cone" model (solid curve) for the model parameter value ω = 24.75° [23]. The depth-dose curves calculated in the SEM2N model with the model parameters: Q_n =1, α_n = 0.36 (curve 1); Q_n =1, α_n = 0.09 (curve 2), and Q_n =1, α_n = 0.23 (dashed curve) are displayed in Fig. 5 for comparison.

One can see from Fig. 5, that the results obtained in the "Cone" model are in good agreement with those obtained in the SEM2N model for the parameters (Q_n =1, α_n = 0.23). Note that the results obtained in the "Cone" model coincide with the results obtained in the SEM2U model for the model parameters (Q_u = 1, α_u=0.46). Calculations of the depth-dose curves for different beam incidence angles θ < 60° show that there is satisfactory agreement between the results obtained in the "Cone" model and in the SEM2N model, if one assumes that the model parameter Q_n =1, and the value of the parameter α_n is determined by the value of the "Cone" model parameter: α_n = 0.5*tan(ω).

The results obtained from comparing the "Cone" model with the SEM2U and SEM2N models indicate that, at a qualitative level, there is agreement between the results obtained in the SEM2N model and the SEM2U model. Numerical

comparison of depth-dose curves calculated using these models demonstrate that the calculation results are in good agreement for angles $\theta < 60°$ if the model parameters are linked by the following relations: $Q_n = Q_u$ and $\alpha_n = 0.5*\alpha_u$.

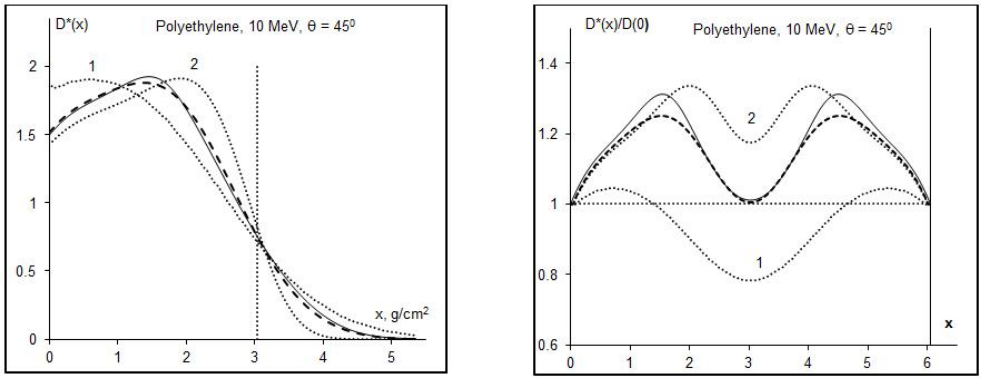

Figure 5. Depth-dose curves in a semi-infinite medium (left) and in a layer of optimal thickness $H_{opt} = 6.06$ g/cm^2 with two-sided irradiation (right).

The depth-dose curves in the layer of optimal thickness under two-sided electron irradiation, calculated in the "Cone" model and in the SEM2N model, are shown in Fig. 6. The parameter of the "Cone" model is chosen as $\omega = 24.75°$ (solid curve). And for the SEM2N model the following model parameters are chosen: $Q_n = 1$, $\alpha_n = 0.23$ (dashed curve), and $Q_n = 1.1$, $\alpha_n = 0.27$ (dotted curve). The depth-dose curve calculated using the Monte Carlo method is presented by solid red curve for comparison.

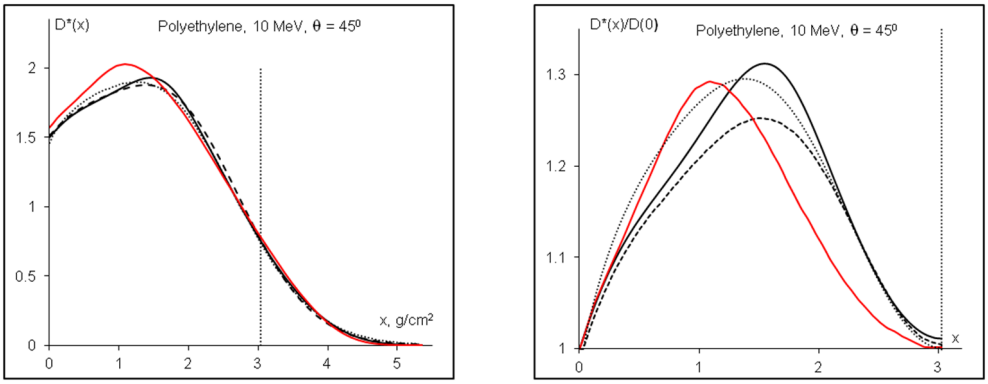

Figure 6. Depth-dose curves calculated for a semi-infinite medium (left) and for a layer of optimal thickness $H_{opt} = 6.06$ g/cm^2 with two-sided irradiation (right).

One can see in Fig. 6, that the depth-dose curve calculated by the SEM2N model can correctly describe both the value of the optimal layer thickness and the uniformity of the dose distribution in the layer. This follows from the fact that the maximum value of the dotted curve is close to the maximum value of the dose in the layer calculated by the Monte Carlo method, and the minimum value equal to 1 is in the middle of the layer of optimal thickness. Thus, the two-parameter SEM2N model provides the possibility to calculate a depth-dose curve that can simultaneously describe two technological characteristics of the radiation sterilization process – the optimal layer thickness and the uniformity of the dose distribution in the layer.

CONCLUSIONS

The spatial distribution of transferred energy in the volume of a target, initiated by the normal incidence of a point beam of radiation on the surface of a semi-infinite medium, is used as a basic object (Dose-Map object) for the development of computer dosimetry models. For a two-parameter approximation of the Dose-Map object, three-dimensional geometric figures are suggested, whose surfaces are formed by rotating the plots of power functions around the abscissa axis.

The two-parameter semi-empirical models of the object are designed on the base of two assumptions. First, the Dose-Map object has axial symmetry relative to the direction of the radiation particle incidence on the target. Second, the dose spatial distribution is uniform or normal (Gaussian distribution) in the ***Dose-Map*** object cross sections at all the depths.

Semi-empirical models SEM2U and SEM2N are developed for calculating the depth-dose curves from radiation incident on the target at the angle θ. Doing this, the following assumption is applied. The parameters of the Dose-Map object in its eigen coordinate system do not change with a change in the beam incidence angle θ.

Expressions for calculating the depth-dose curves from radiation incident on the target at the angle θ are obtained in the form of the integral transformation of the depth-dose curve known for normal incidence of the radiation beam on the

target. Software is produced for calculating the depth-dose curves in a semi-infinite medium with uniform irradiation of the medium surface by the electron beam.

Satisfactory agreement is established between the results obtained using the developed herein semi-empirical models SEM2U and SEM2N and the results obtained in the semi-empirical model "Cone" and Monte Carlo modeling of depth-dose curves at different incidence angles of the electron beam on the target.

Examples are provided for which the developed two-parameter models make it possible to simultaneously and consistently describe two technological characteristics of the two-sided irradiation process: the optimal target thickness and the dose uniformity coefficient in the target. Consistent data regarding these characteristics allow for the reasonable choice of optimal electron beam irradiation modes for radiation sterilization.

The present paper describes in detail the procedure of developing the semi-empirical models for calculating the depth-dose curves of the electron beam in a semi-infinite medium. The described approach to developing the semi-empirical models can be further applied to developing models for computer dosimetry of other types of penetrating radiation, for example, bremsstrahlung or gamma quanta, which are widely, used nowadays as penetrating radiation for radiation technologies.

ORCID

Igor O. Girka, https://orcid.org/0000-0001-6662-8683; **Valentín T. Lazurik,** https://orcid.org/0000-0002-8319-0764

REFERENCES

[1] S. Schiller, U. Heisig, and S. Panzer, *Electron Beam Technology*, (John Wiley & Sons Inc, 1995).
[2] M. Reiser, *Theory and Design of Charged Particle Beams*, (John Wiley & Sons, 2008).
[3] R.C. Davidson, and H. Qin, *Physics of Intense Charged Particle Beams in High Energy Accelerators*, (World Scientific, Singapore, 2001).
[4] ICRU REPORT 35, *Radiation dosimetry: electron beams with energies between 1 and 50 MeV*, (ICRU, 1984), p. 168.
[5] R.J. Woods, and A.K. Pikaev, *Applied radiation chemistry: radiation processing*, (Wiley, New York, 1994).
[6] ISO/ASTM Standard 51649, *Practice for dosimetry in an e-beam facility for radiation processing at energies between 300 keV and 25 MeV*, (ASTM Standards, vol. 12.02, 2005).
[7] Yu. Pavlov, and P. Bystrov, Radiation Physics and Chemistry, **196**, 110110 (2022). https://doi.org/10.1016/j.radphyschem.2022.110110
[8] Z. Zimek, Radiation Physics and Chemistry, **189**, 109713 (2021), https://doi.org/10.1016/j.radphyschem.2021.109713
[9] S. Howard, and V. Starovoitova, Applied Radiation and Isotopes, **96**, 162 (2015). https://doi.org/10.1016/j.apradiso.2014.12.003
[10] R. Pomatsalyuk, S. Romanovskyi, V. Shevchenko, and V. Uvarov, Problems of Atomic Science and Technology, (5), 131 (2024). https://doi.org/10.46813/2024-153-131
[11] R.I. Pomatsalyuk, S.K. Romanovsky, V.O. Shevchenko, V.Yu. Titov, D.V. Titov, and V.L. Uvarov, Problems of Atomic Science and Technology, (5), 117 (2024). https://doi.org/10.46813/2024-153-117
[12] ASTM E2232-21 *Standard Guide for Selection and Use of Mathematical Methods for Calculating Absorbed Dose in Radiation Processing Applications*, (ASTM, 2021), p. 19. https://doi.org/10.1520/E2232-21
[13] F. Salvat, J. Fernandez-Varea, J. Sempau, *PENELOPE 2011: A Code System for Monte Carlo Simulation of Electron and Photon Transport*, (Nuclear Energy Agency, 2012), p. 385.
[14] S.-T. Jung, S.-H. Pyo, W.-G. Kang, Y.-R. Kim, J.-K. Kim, C.M. Kang, Y.-C. Nho, and J.-S. Park, Radiation Physics and Chemistry, **186**, 109506 (2021). https://doi.org/10.1016/j.radphyschem.2021.109506
[15] M. Rezzoug, M. Zerfaoui, Y. Oulhouq, A. Rrhioua, S. Didi, and D. Bakari, Radiation Physics and Chemistry, **235**, 112828 (2025). https://doi.org/10.1016/j.radphyschem.2025.112828
[16] D.J.S. Findlay, Nucl. Instrum. Methods A, **276**(3), 598 (1989). https://doi.org/10.1016/0168-9002(89)90591-3
[17] V.L. Uvarov, A.A. Zakharchenko, N.P. Dikiy, Yu.V. Lyashko, R.I. Pomatsalyuk, V.A. Shevchenko, and Eu.B. Malets, Problems of Atomic Science and Technology, (6), 180 (2023). https://doi.org/10.46813/2023-148-180
[18] V.L. Uvarov, A.A. Zakharchenko, N.P. Dikiy, R.I. Pomatsalyuk, and Yu.V. Lyashko, Applied Radiation and Isotopes, **199**, 110890 (2023). https://doi.org/10.1016/j.apradiso.2023.110890
[19] V.G. Rudychev, M.O. Azarenkov, I.O. Girka, V.T. Lazurik, and Y.V. Rudychev, Radiation Physics and Chemistry, **206**, 110815 (2023). https://doi.org/10.1016/j.radphyschem.2023.110815
[20] V.L. Uvarov, A.A. Zakharchenko, N.P. Dikiy, YuV. Lyashko, and R.I. Pomatsalyuk, Radiation Physics and Chemistry, **214**, 111547 (2024). https://doi.org/10.1016/j.apradiso.2024.111547
[21] V.G. Rudychev, V.T. Lazurik, and Y.V. Rudychev, Radiation Physics and Chemistry, **186**, 109527 (2021). https://doi.org/10.1016/j.radphyschem.2021.109527
[22] M. Rosenstein, H. Eisen, and J. Silverman, Journal of Applied Physics, **43**, 3191 (1972). https://doi.org/10.1063/1.1661684
[23] V. Lazurik, S. Sawan, V. Lazurik, and O. Zolotukhin, in: *4th International Maghreb Meeting of the Conference on Sciences and Techniques of Automatic Control and Computer Engineering Proceedings*, (IEEE, Maghreb, 2024), pp. 649–653. https://doi.org/10.1109/MI-STA61267.2024.10599694
[24] I. Melnyk, A. Pochynok, and M. Skrypka, System Research and Information Technologies, (4), 133 (2024). https://doi.org/10.20535/SRIT.2308-8893.2024.4.11
[25] S.V. Denbnovetsky, V.I. Melnik, I.V. Melnik, and B.A. Tugay, in: *XVIII-th International Symposium on Discharges and Electrical Insulation in Vacuum Proceedings*, (IEEE, Eindhoven, 1998), pp. 637-640. https://doi.org/10.1109/DEIV.1998.738530
[26] I.V. Melnik, and B.A. Tugay, Radioelectronics and Communications Systems, **55**, 514 (2012). https://doi.org/10.3103/S0735272712110064
[27] V. Lazurik, S. Sawan, V. Lazurik, and V. Rudychev, in: *3rd International Maghreb Meeting of the Conference on Sciences and Techniques of Automatic Control and Computer Engineering Proceedings*, (IEEE, Maghreb, 2023), pp. 25–29. https://doi.org/10.1109/MI-STA57575.2023.10169519

[28] T. Tabata, P. Andreo, and K. Shinoda, Radiation Physics and Chemistry, **53**, 205 (1998). https://doi.org/10.1016/S0969-806X(98)00102-9

НАПІВЕМПІРИЧНІ МОДЕЛІ КЕРУВАННЯ ЕЛЕКТРОННИМ ПРОМЕНЕМ ДЛЯ РАДІАЦІЙНОЇ СТЕРИЛІЗАЦІЇ

Ігор О. Гірка, Валентин Т. Лазурик

Харківський національний університет імені В. Н. Каразіна, Харків, Україна

Для проведення радіаційної стерилізації необхідно визначати допустимі режими опромінення, що здійснюється за допомогою методів комп'ютерної дозиметрії. На сьогодні вибір оптимальних режимів опромінення може ґрунтуватися на моделях кривої залежності дози від глибини при різних кутах падіння електронного пучка на шар речовини. У цій роботі для розробки таких моделей використано розподіл переданої енергії в об'ємі мішені, ініційований нормальним падінням точкового пучка випромінювання на поверхню напівбезкінечного середовища (об'єкт Dose-Map). Напівемпіричні моделі об'єкта Dose-Map розроблені на основі двох припущень. Одна з них полягає в тому, що мішень має осьову симетрію відносно напрямку падіння частинок випромінювання на мішень. Друге полягає в тому, що просторовий розподіл дози є рівномірним або нормальним (розподіл Гауса) у поперечних перерізах об'єкта Dose-Map на всіх глибинах. Для двопараметричної апроксимації об'єкта Dose-Map запропоновано тривимірні геометричні фігури, поверхні яких утворюються обертанням графіків степеневих функцій навколо осі абсцис. Напівемпіричні моделі розроблені на основі припущення, що параметри об'єкта Dose-Map у його власній системі координат не змінюються при зміні кута падіння променя. Отримано вирази для розрахунку кривих глибинної дози від випромінювання, що падає на мішень під кутом θ, у вигляді інтегрального перетворення кривої глибинної дози для нормального падіння пучка випромінювання на мішень. Розроблено програмне забезпечення для розрахунку кривих залежності дози від глибини в напівбезмежному середовищі при рівномірному опроміненні електронним пучком. Тестово реалізовані алгоритми розрахунку кривих залежності дози від глибини від електронного пучка, що падає на мішень під кутом θ. Встановлено задовільну узгодженість між результатами, отриманими за допомогою розроблених напівемпіричних моделей, та результатами моделювання методом Монте-Карло кривих залежності дози від глибини при різних кутах падіння електронного променя на мішень. Встановлено добру узгодженість між результатами, отриманими за допомогою напівемпіричної моделі "Конус", та результатами, отриманими за допомогою розроблених двопараметричних напівемпіричних моделей SEM2U та SEM2N. За допомогою числових методів досліджено можливості розроблених двопараметричних моделей для більш повного опису технологічних характеристик процесу радіаційної стерилізації. Наведено приклади, де розроблені двопараметричні моделі дають можливість одночасно описувати дві технологічні характеристики процесу двостороннього опромінення: оптимальну товщину мішені та коефіцієнт рівномірності дози (DUR) у мішені. Узгоджені дані щодо цих характеристик дають можливість обґрунтовано вибирати оптимальні режими опромінення електронним променем під час радіаційної стерилізації. Зазначено можливості використання запропонованого в цій статті підходу для розробки набору напівемпіричних моделей комп'ютерної дозиметрії процесів опромінення в радіаційних технологіях.

Ключові слова: *дозиметрія електронного пучка; крива глибинної дози; процеси стерилізації; контроль оптимальних режимів; напівемпірична модель; метод Монте-Карло*